ELSEVIER

Journal of Nuclear Materials 266–269 (1999) 1202–1206

journal of nuclear materials

Kinetic modeling of the transport in the SOL of TdeV during LH current drive and ELM bursts

M. Shoucri [a,*], I. Shkarofsky [a], J.-L. Gauvreau [a], P. Jacquet [a], G. Pacher [a], R. Decoste [a], O. Batishchev [b,1], A. Batishcheva [b], D. Sigmar [b]

[a] *Centre Canadien de Fusion Magnétique, Varennes, Que., Canada J3X 1S1*

[b] *Massachusetts Institute of Technology PSFC, Cambridge, MA 02139, USA*

Abstract

Fully kinetic plasma–neutrals Fokker–Planck code ALLA is used to simulate the transport properties of the scrape-off layer (SOL) plasmas of Tokamak-de-Varennes during lower hybrid (LH) current drive and edge localized modes (ELM) bursts. During LH heating a sizable amount of auxiliary power which is directly deposited into the SOL plasma makes it semi-collisionless. This energy is convected along open magnetic lines directly to the plates, and may be responsible for the hot spots formation. During Type III ELM bursts the detached SOL plasma reattaches to the divertor plates. We find that electron, ion and neutral atom distribution functions are non-Maxwellian for the modeled transient regimes under typical conditions of TdeV SOL plasmas.

Keywords: ELM; LHCD; Numerical simulations

1. Introduction

Tokamak-de-Varennes (TdeV) is a mid-size divertor tokamak with major and minor radii 87 and 25 cm, respectively. It operates with relatively low density ($n_P \sim 10^{13}$ cm^{-3}) and hot ($T_P \approx 30$ eV) plasmas in the scrape-off layer (SOL) [1,2]. In the experiments described below, it was operated in an upper single null configuration, with plasma current 140 kA $\leqslant I_P \leqslant$ 190 kA and toroidal magnetic field 1.5 T $< B_T <$ 1.9 T. Typical TdeV SOL mean plasma density and temperatures are $n_P \approx 0.5 \times 10^{13}$–$1 \times 10^{13}$ cm^{-3} and $T_P \approx$ 10–20 eV, respectively. The ratio of the Coulomb mean-free path λ (cm) $\approx 10^{12} T_P^2$ (eV)$/n_P$ (cm^{-3}) to half the magnetic field connection length $L = 10^3$ cm is 0.02–0.05 for the line averaged TdeV SOL plasma parameters. This means that the electron distribution can be equilibrated for thermal particles with energies less than T_P, but can still depart from a Maxwellian for suprathermal electrons with energies higher than $3T_P$. The heat flux parallel to the magnetic field is carried mostly by the suprathermal electrons with energy $E \geqslant 3T_P$. A small change in the hot electron population can cause a significant change in the SOL plasma flow because these electrons affect the Spitzer–Harm conductivity, and the plasma–neutral-particles interaction rates. Sheath potential magnitude at the plates and particle and energy fluxes on the divertor depend strongly on the details of the electron and ion distribution functions. Also rates of neutral atoms ionization and of impurity and neutrals excitation in the relatively cold divertor region are determined by the tail of the electron distribution function. Thus, the presence of an elevated electron tail may cause a significant increase in the impurity radiation.

The kinetic effects may be additionally amplified during certain transient effects in the SOL, which were observed in the TdeV experiments. The first group of effects is related to the lower-hybrid (LH) heating adopted on the machine. The formation of the hot spots around the strike point was observed during LH heating of the electrons. This observation suggests that a signi-

* Corresponding author. Tel.: +1-514 652 8723; fax: +1-514 652 8625; e-mail: shourci@ccfm.ireq.ca

[1] Also at Lodestar Research Corporation, Boulder, USA, and Moscow Physical-Technical Institute and Keldysh Institute for Applied Mathematics, Moscow, Russian Federation.

PII: S 0 0 2 2 - 3 1 1 5 (9 8) 0 0 8 6 0 - 5

ficant amount of power can be deposited directly into the SOL plasma causing a rise of its temperature, and thus, making it less collisional.

All these important, but quite complex phenomena can be studied correctly only with time-dependent kinetic code. We apply our 1D2V Fokker–Planck code ALLA [3] to address kinetic effects during transient regimes in the TdeV SOL plasma. The kinetic model for plasma and neutral particles is presented in Section 2. In Section 3 we will present the results for the LH simulations and Section 4 will present results for the edge localized mode (ELM) bursts' simulations. Main results will be listed in Section 5.

2. Physical model and equations

The plasma particles and neutral atoms mixture is described by a set of non-linear equations, which are strongly coupled via collisions, electric field and boundary conditions. The following three kinetic equations (in 1D2V approximation, which neglects 2D effects, like important anomalous cross-field transport) describe the evolution of the distribution functions $f_s(t,x,v,\mu)$ of different species:

$$\frac{\partial f_e}{\partial t} + v\mu\frac{\partial f_e}{\partial x} - \frac{eE_x}{m_e}\frac{\partial f_e}{\partial v_x} = C_{ee} + C_{ei} + C_{EX} + C_I - S_e, \quad (1)$$

$$\frac{\partial f_i}{\partial t} + v\mu\frac{\partial f_i}{\partial x} + \frac{eE_x}{m_i}\frac{\partial f_i}{\partial v_x} = C_{ii} + C_{EX} + C_I - S_i, \quad (2)$$

$$\frac{\partial f_n}{\partial t} + v\mu\frac{\partial f_n}{\partial x} = C_{nn} - C_I + S_n, \quad (3)$$

where $s =$ e,i, or n marks electrons, ions, and neutrals, respectively; $\mu = v_\parallel/v$ is a pitch angle, $v^2 = v_\parallel^2 + v_\perp^2$ the square of total velocity, and $v_x = v_\parallel$ the velocity parallel to the magnetic line; C_{ee}, C_{ei}, C_{ii} are e–e, e–i, and i–i Coulomb collisions terms, respectively, C_{EX} and C_I are neutral excitation and ionization terms, respectively; C_{nn} term represents elastic neutral–neutral collisions; S_e, S_i and S_n are boundary mass sources due to surface recombination and neutral recycling. These equations are solved using a splitting scheme [4]. The self-consistent parallel ambipolar electric field E_x is calculated from the charged particles parallel momentum balance equation with a correction to assure quasi-neutrality [5]. Although the sheath structure is not resolved at the plate because the spatial dimension is much bigger than the Debye length, the sheath potential drop at the plate $\Delta\phi_{sh}$ is evaluated from the logical sheath boundary condition. We equate the ion flux to the collected electron flux:

$$Z_i n_i c_S(t, x=0) = \int_{-1}^{0}\int_{0}^{v_r} \mu v^3 f_e(t, x=0, v, \mu)\,dv\,d\mu, \quad (4)$$

where $v_r^2 = 2e\Delta\phi_{sh}/m_e$, Z_i is the effective ion charge number (we use $Z_i = 1$ in current simulations) and c_S is a the local sound speed. The outflux of cold neutrals ($T_n = 1$ eV) with a half-Maxwellian distribution is equal to the plasma flux onto the wall (100% neutral recycling). More details about numerical methods and procedures may be found in Ref. [5].

3. Transport in the SOL of TdeV during LH current drive

The 1 MW LH current drive system of TdeV operates at 3.7 GHz and its multijunction antenna generates a spectrum of $N_\parallel$ adjustable between 2.0 and 3.3. During LH current drive in TdeV, the antenna is located in the SOL. The measurements indicate that a sizable fraction of an RF energy is deposited directly into the SOL plasma electrons resulting in a distribution function with an elongated tail with energies up to few keV. This fraction of RF power is dissipated directly in a thin plasma layer of ~1 cm just in front of the antenna, and fast electrons created there follow the open field lines to the divertor plates, forming noticeable hot spots [1,2]. In the present simulation, the electron distribution function at the equatorial plane is taken from the modeling results presented in Ref. [7]. The lower energy limit of the fast electrons was taken to be $E \sim 200$ eV, and the upper energy limit was taken to be around 5 keV. The results of the kinetic simulation show the impact of the almost collisionless energetic tail at the midplane caused by LH heating, on the TdeV SOL plasma conditions. Fig. 1 follows the variation of the profile of the electron temperature T_e and shows how the LH energy deposited at $x = 10^3$ cm propagates to the divertor plate. It takes approximately 1 μs for the first energetic particles gen-

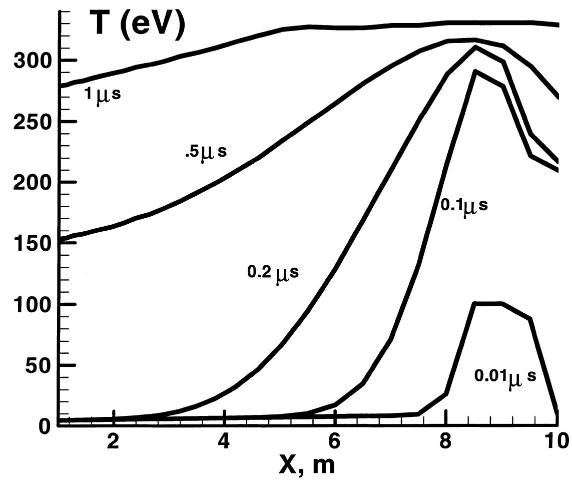

Fig. 1. Time evolution of the electron temperature profile after switching RF power on.

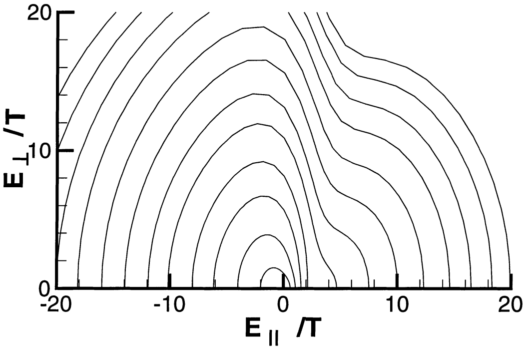

Fig. 2. Electron distribution function F_e at the divertor 1 μs after switching on RF power.

erated at the equatorial plane to reach the divertor plate. Fig. 2 shows the distribution function of the electrons at the divertor plate after the arrival of the energetic tail at $t = 1$ μs. It shows the presence of energetic particles generated in the plateau of the distribution function in the equatorial plane. We note that before LH heating the electron distribution was Maxwellian.

4. Transport in the SOL of TdeV during ELM bursts

Type III ELM bursts on TdeV were observed during H mode operation. The H mode was obtained during EC injection (500 kW power at $2\omega_{ce}$ or 110 GHz). The ELM's modulation is monitored by following the D_α radiation at the equatorial plane. The density at the separatrix was 10^{13} cm^{-3}. The ELM's modulation was simulated by a variation of the incoming anomalous heat flux into the half of the open magnetic line on the equatorial side. This anomalous heat flux was modeled by a diffusion in the perpendicular component of the electron velocity whose period was taken from the experimental results (for shot # 31 952), and whose magnitude was tailored to reproduce the magnitude of the observed modulation in the shot 31 952. Namely, the mean heating power of about 600 kW was increased by a factor of 4 during each of several consecutive ELM bursts. The duration of the heat pulse was 0.6 ms and the period of these pulses was 2 ms to match the experimental observations. We had no particle (mass) flux because there is no central fueling in the TdeV, and because we have assumed 100% recycling of neutrals at the walls. In Fig. 3, four traces of the electron (a) and ion (b) temperatures are presented. They correspond to different spatial positions: equatorial plane (E), the midplane (M), close to the X-point (X), and the divertor plate (D). The figure also shows the evolution of the neutral density and the plasma density (c). We note the ion temperature at the divertor plate decreasing at the beginning of every pulse. This is due to the fact that

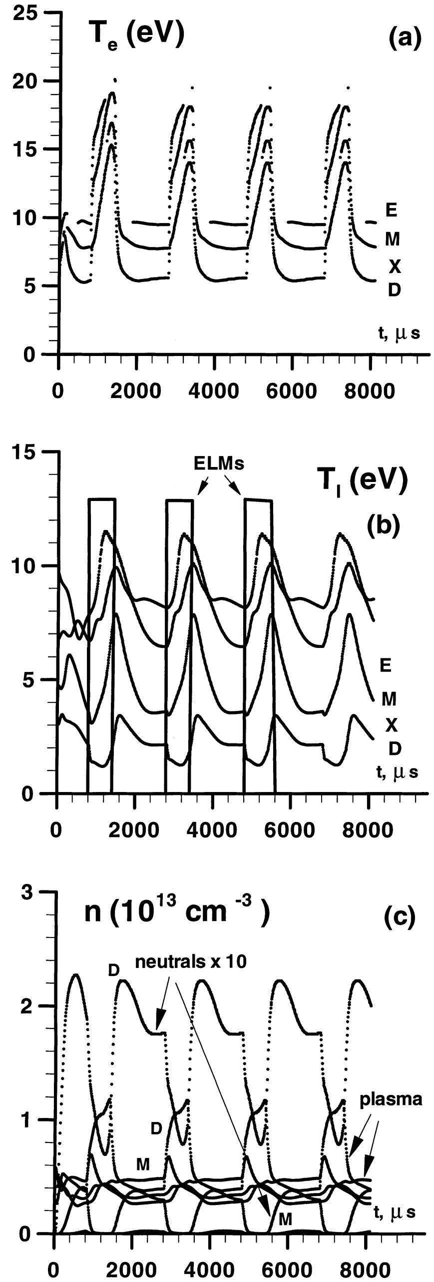

Fig. 3. (a) Time evolution of the electron temperature during ELM bursts at four different locations: equatorial plane (E), midplane (M), X-point (X) and divertor plate (D). (b) Time evolution of the ion temperture during ELM burts at four different locations: equatorial plane (E), midplane (M), X-point (X) and divertor plane (D). (c) Time evolution of the neutral and plasma densities during ELM bursts at different locations.

neutrals, when ionized, give a cold contribution to the ion population. Also when the electrons are strongly heated at the beginning of the pulse, the equilibration time with ions gets longer ($\sim T_e^{1.5}$). The plasma, which was detached before the pulse, is temporarily attached to the plate during the ELM burst. This results in an increased plasma density at the divertor plate as we can see from Fig. 3. The distribution functions at the divertor plate at $t = 1.4$ ms (at the end of the heating pulse) are presented in Fig. 4 for electrons (e), ions (i) and neutrals (n). It illustrates a noticeable deviation of the distribution functions from a Maxwellian. As can be seen, the ions are strongly accelerated by the ambipolar electric field up to local sound speed. The tail of the electron distribution is cut-off by the enhanced sheath potential which absorbs the energetic electrons, and reflects back all the electrons with energies $E \leqslant e\Delta\phi_{sh}$. This results in the distribution function being depleted for high positive velocities. Neutral density is relatively low and neutral collisionality (as defined by C_{nn} term in Eq. (3)) is insufficient to Maxwellize the neutral distribution. Fig. 4(n) shows the neutral distribution function during a minimum of the neutral density at the end of the heating pulse. Fig. 5 shows the corresponding distribution functions at the X-point. One can see that the sheath potential has an increased value (cut-off tail of the electron distribution with large $v_{\|}$). Ion distribution

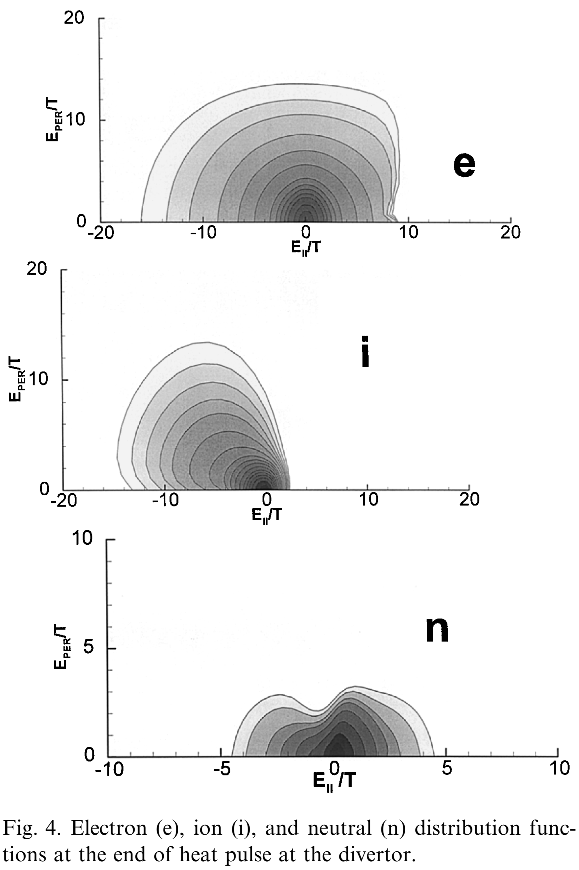

Fig. 4. Electron (e), ion (i), and neutral (n) distribution functions at the end of heat pulse at the divertor.

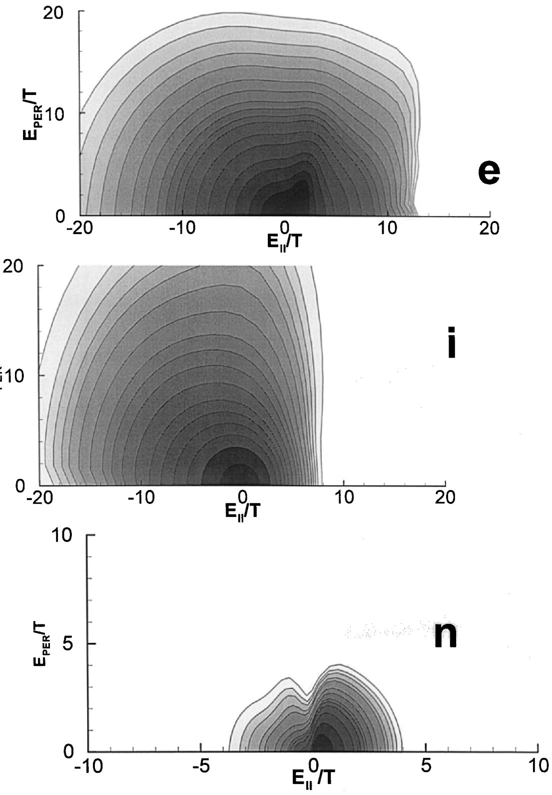

Fig. 5. Electron (e), ion (i) and neutral (n) distribution functions at the end of heat pulse at the X-point.

function is more non-Maxwellian (compared to X-point), and is characterized with visibly higher drift velocity near the plate. The distribution function of neutrals is more equilibrated where the neutral density is highest (see Figs. 4(n) and 5(n)). Of course, found by kinetic simulation, the significant departures of the plasmas and neutral particles' distribution functions from equilibrium result in drastic changes of plasma transport coefficients and plasma–neutral interaction rates. We will analyze these important kinetic effects in full detail in our future work.

5. Conclusions

A non-Monte-Carlo (statistical fluctuations free) Fokker–Planck code ALLA [3,6] for electrons, ions and neutral atoms, which includes some of the most important collisional processes in plasma, has been applied to study transport processes in the SOL of TdeV during Lower Hybrid current drive and Type III Edge Localized Modes bursts. Our fully kinetic simulations show that during LH heating the sizable amount of RF power, deposited directly into the SOL plasma, changes the plasma conditions from semi-collisional to collisionless with $\lambda \geqslant L$. The electron distribution in the whole SOL region is characterized with LH plateau, because of weakened e–e Coulomb collisions. A big fraction of RF power is carried by the particles with energies $E \sim 0.5$ keV from the RF antenna along the open magnetic line to the strike point.

Type III ELM simulations showed several interesting kinetic features. First, during ELM burst cold detached plasma reattaches to the divertor plates. Plasma density rises, while neutral density drops in the divertor. Interestingly, ion temperature drops too. It requires 1 ms (or about half of ELM duration period) for plasma temperature and density to become quasi-steady-state after ELM propagation. However, electron and ion distribution functions do not equilibrate during both ELM bursts and in the period between them. The neutral atoms distribution near the wall is not Maxwellian due to the insufficient neutrals density.

Acknowledgements

The CCFM is funded by Hydro-Quebec and the Institut national de la recherche scientofique. Work is supported by US DoE contracts no. DE-FG02-97ER-54392 at Lodestar Research Corporation and no. DE-FG02-91ER-54109 at MIT PSFC.

References

[1] R. Decoste et al., Plasma Phys. Control. Fusion 38 (1996) A121.
[2] B. Stansfield et al., J. Nucl. Mater. 241–243 (1997) 739.
[3] A.A. Batishcheva et al., Phys. Plasmas 3 (1996) 1634.
[4] M. Shoucri et al., Contr. Plasma Phys. 38 (1998) 225.
[5] O.V. Batishchev et al., Phys. Plasmas 4 (1997) 1672.
[6] O.V. Batishchev et al., Proc. 16th Int. Conf. Num. Sim. Plas. (1998) 155; J. Plasma Phys., accepted for publication.
[7] J.M. Mailloux et al., J. Nucl. Mater. 241–243 (1997) 745.